Electronic properties of boron doped single-layer graphene

Roman S. Tikhonov, and Egor P. Sharin

Citation: AIP Conference Proceedings **2041**, 020020 (2018); doi: 10.1063/1.5079351
View online: https://doi.org/10.1063/1.5079351
View Table of Contents: http://aip.scitation.org/toc/apc/2041/1
Published by the American Institute of Physics

Electronic Properties of Boron Doped Single-Layer Graphene

Roman S. Tikhonov[a] and Egor P. Sharin

Theoretical Physics Department, North-Eastern Federal University, 58 Belinsky Str., Yakutsk, 677000 Russia

[a]Corresponding author: ep.sharin@s-vfu.ru

Abstract. Structural and electronic properties of single-layer graphene doped with boron atoms with varying doping concentrations and configurations have been investigated here via first-principles density functional theory calculations. It was found that a band gap increases with an increase in the doping concentration. It was observed that the band gaps also depend on the atomic configurations considered for substitutional dopants. Electronic structures of B-doped graphene systems were also found to be strongly influenced by positioning of the dopant atoms in a graphene lattice. These results indicate an ability to adjust the band gap as required using the B atoms according to a choice of a supercell, i.e., the doping density and substitutional dopant sites, which could be useful in design of graphene-based electronic and optical devices.

INTRODUCTION

Graphene, a single layer of carbon atoms arranged in a honeycomb lattice, has been a focus of recent research efforts [1, 2, 3] due to its unique semimetallic zero-gap electronic structure. The unusual structural and electronic properties make graphene a promising material for nanoelectronics. Graphene does not have an essential function for controlled and reliable operation of transistors, namely, the band gap near the Fermi level. Several schemes have been proposed to open the band gap in graphene. Chemical functionalization [4, 5, 6, 7, 8, 9] is an alternative way to manipulate the electronic properties of graphene. A promising approach to a controlled change of the electronic properties of graphene is to alloy it with foreign atoms (similar to the widely known approach in silicon electronics). It is known, that when introducing the boron atoms into graphene, it can be converted into a p-type semiconductor and also cause a forbidden band appearance [10, 11]. A possibility of management of the type and concentration of charge carriers in graphene opens up broad prospects for development of new biosensors [12], lithium batteries [13] and fuel elements [14].

CALCULATION METHOD

In this work, we used a first-principles band calculation technique based on the density functional theory. We used Quantum Espresso, which is a first-principles calculation code with high precision using a plane wave method. We adopted a generalized gradient approximation (GGA) as a term exchange correlation with a cutoff energy of 450 eV and all calculations were performed nonmagnetically. The generalized gradient approximation (GGA) exchange-correlation (XC) functional in the Perdew-Burke-Ernzerhof (PBE) form [15] is adopted in the structural optimization and electronic structure calculations of different doped graphenes. The algorithm has used the Rappe-Rabe-Kaxiras-Joannopoulos (RRKJ) model of ultra- soft pseudo-potentials to take into account the interaction between the ion cores and valence electrons. The unit cell for a graphene sheet adopted a 3×3 structure. A lattice constant of the graphene used a value optimized by calculation. Further, in order to minimize the interactions between two adjacent graphene layers, a vaccum distance of 15 Å is maintained in the calculations. Sampling of the Brillouin zone is performed using the k-point mesh generated by the Monkhorst-Pack scheme [16]. Converged k-point grids corresponding to a 16×16×1 grid for the graphene unit cell are used for different graphene supercells. For all systems, relaxation of basis vectors and atomic coordinates is performed by minimizing the total energy. The structural optimization has been

2D Systems of the Strong Correlated Electrons: From Fundamental Research to Practical Applications
AIP Conf. Proc. 2041, 020020-1–020020-4; https://doi.org/10.1063/1.5079351
Published by AIP Publishing. 978-0-7354-1767-0/$30.00

conducted using the Broyden-Fletcher-Goldfard-Shanno (BFGS) minimization until residual forces on the atoms are lower than 0.003 eV/Å.

RESULTS AND DISCUSSION

We carry out our calculations with the different concentrations of B doping (5.56% , 11.11%, 16.66% and 22.23%) in graphene and also take into account the different sites of doping for the same concentration. The boron atom is likely to adjust to surrounding C atoms of the host. When the graphene sheet is doped with one boron atom, the boron atom also undergoes sp^2 hybridization and due to the nearly same size of C and B, no significant distortion in 2-D structure of graphene is expected, except for the change in adjoining bond length (see Fig. 1(a)). Upon the structural optimization of graphene, the supercell doped with one B atom remains slightly disturbed. The optimized lattice constant increases from 2.458 Å to 2.463 Å for the 3×3 supercell doped with one B atom. Using the computational procedure as stated above, it is possible to calculate the electronic properties, especially the band structure. The K-points along special directions of Brillouin zone are of interest and we find that the linear dispersion near the Dirac point is not destroyed Fig. 1(b).

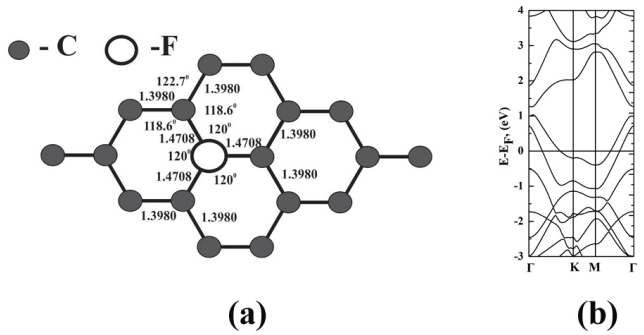

FIGURE 1. Optimized geometry and band band structure of single B atom doped graphene sheet. C and F atoms are presented by black and light circles (balls). Distances between atoms are given in angstroms.

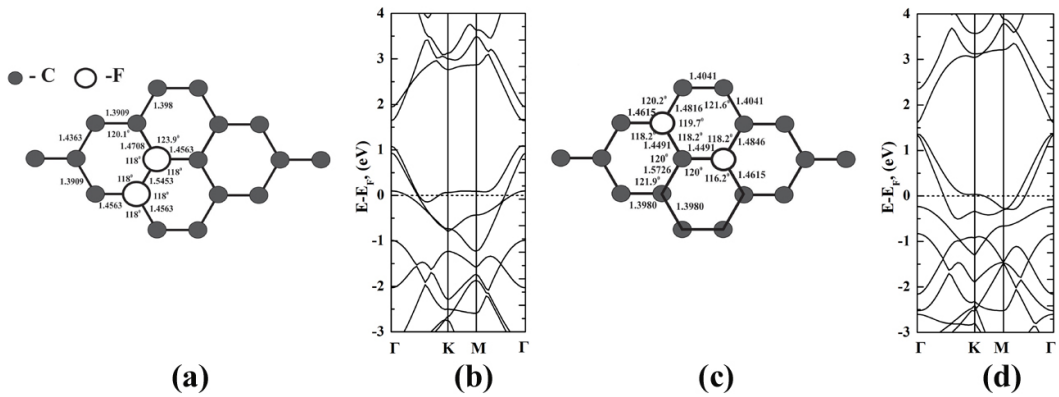

FIGURE 2. Optimized geometry and band band structure of single B atom doped graphene sheet. C and F atoms are presented by black and light circles (balls). Distances between atoms are given in angstroms.

Figure 2 show the optimized geometry and band structure of two B atom doped graphene sheet. The optimized lattice constant increases from 2.458 Å to 2.509 Å for the 3×3 supercell doped with two B atoms. The investigations of the structural properties show shrinkage of the C-C bond length in case of B due to the longer C-B bond because of a larger covalent radius of boron than the one of carbon. This also results in disorder of the lattice when the dopants are placed at adjacent positions. The data regarding changes in bond lengths can be read from the structural part of the figures on the left are presented. It may be mentioned that the results regarding bond length alteration are in general consistent with earlier calculations of doping.

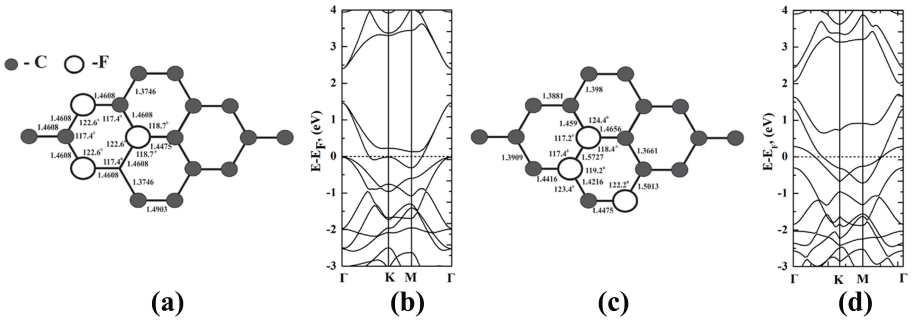

FIGURE 3. Optimized geometry and band band structure of single B atom doped graphene sheet. C and F atoms are presented by black and light circles (balls). Distances between atoms are given in angstroms.

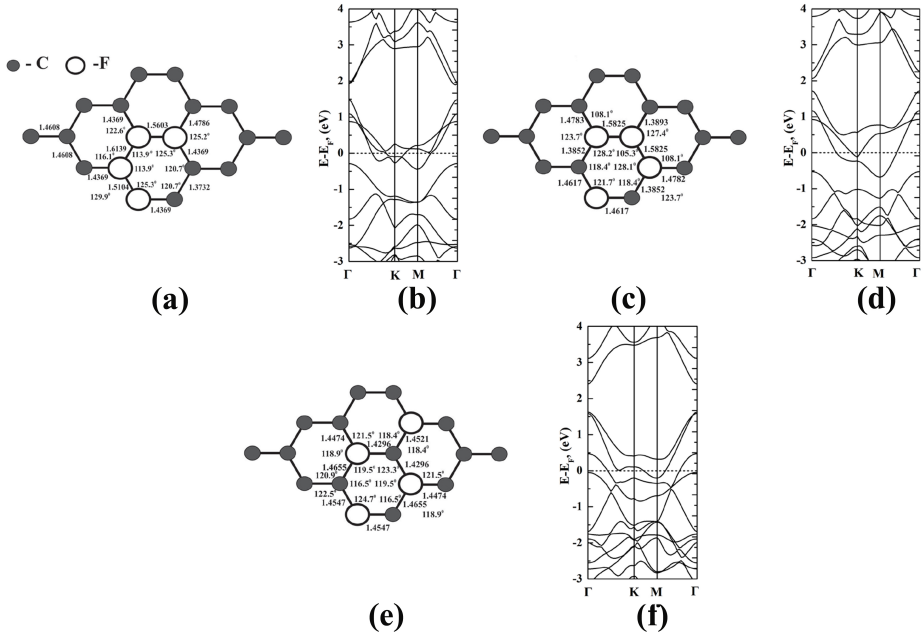

FIGURE 4. Optimized geometry and band band structure of single B atom doped graphene sheet. C and F atoms are presented by black and light circles (balls). Distances between atoms are given in angstroms.

Here we consider substitution of three C atoms by three B atoms in the 3×3 graphene supercell. Figure 3 (a,c) shows the relaxed geometries of the 3×3 graphene supercell doped with three B atoms at same and adjacent sublattices, respectively. The optimized lattice constant increases from 2.458 Å to 2.533 Å for the 3×3 supercells doped with three B atoms. After the structural optimization, it was found that the graphene structures doped with three B atoms at adjacent locations experience significant geometrical distortion due to the positioning of three B atoms in the same

six-membered carbon ring Fig. 3 (a), as compared to the other graphene systems doped with three B atoms Fig. 3(c). Figure 3(b,d) present the band structure computed for the optimized structures of three B atom doped graphene sheet. The band structures of both 3×3 graphene supercells doped with three B atoms show non-zero band gaps around the Dirac point as seen in Fig. 3(b,d). This changes behavior of graphene from semimetal to conductor. The optimized geometry of four B atom doped graphene sheet is depicted in Fig. 4(a,c,e). Figure 4(a,c,e) present the relaxed structures of the 3×3 supercells doped with four B atoms at adjacent, alternate and same sublattices, respectively.

The graphene systems doped with four B atoms experience the structural distortion when the B atoms (Fig. 4(a,c,e)). The relaxed lattice constant increases from 2.458 Å to 2.578 Å for the 3×3 supercells doped with four B. Figure 4(a,c,e) present the relaxed structures of the 3×3 supercells doped with four B atoms at adjacent, alternate and same sublattices, respectively. The band structures of both 3×3 graphene supercells doped with four B atoms, depicted in Fig. 4(b,d,f), show the non-zero band gap values around the Dirac point. All graphene structures doped with four B atoms exhibit metallic behaviors.

CONCLUSION

The density functional theory was used to study the geometry and electronic structure of the boron doped graphene 3×3 supercell. The effect of doping was investigated by varying the concentrations of dopants from 5.56% to 22.23% and also by considering the different doping sites for the same concentration of the substitutional doping. It was observed that the structure of the crystal lattice is deformed on doping of the graphene sheet. In the case of B doped graphene, the electronic structure results reveal a splitting energy near E_F, which is moved up for all band structures with the different geometries. This indicates a decrease in the number of valence electrons. The band structures of the 3×3 graphene supercell doped with the B atoms show the non-zero band gap values around the Dirac point. The band gap around the Dirac point is maximum when the dopants are placed at the same sublattice positions (A or B). These interesting results provide the possibility of designing the band gap of graphene as per requirements allowing its application in a wide range of electronic devices.

REFERENCES

[1] K. Novoselov, A. Geim, S. Morozov, D. Jiang, M. Katsnelson, I. Grigorieva, S. Dubonos, and A. Firsov, Nature **438**, 197–200 (2005).

[2] K. Novoselov, E. McCann, S. Morozov, V. Falko, M. Katsnelson, U. Zeitler, D. Jiang, F. Schedin, and A. Geim, Nat. Phys. **2**, 177–180 (2006).

[3] Y. Zhang, Y. Tan, H. Stormer, and P. Kim, Nature **438**, 201–204 (2005).

[4] E. Bekyarova, M. Itkis, P. Ramesh, C. Berger, M. Sprinkle, W. de Heer, and R. Haddon, J. Am. Chem. Soc. **131**, 1336–1337 (2009).

[5] S. Sarkar, E. Bekyarova, S. Niyogi, and R. Haddon, J. Am. Chem. Soc. **133**, 3324–3327 (2011).

[6] P. Rani and V. Jindal, RSC Adv. **3**, 802–812 (2013).

[7] S. S. Varghese, S. Swaminathan, K. K. Singh, and V. Mittal, Electronics **5(4)**, 91–127 (2016).

[8] L.S.Panchokarla, K. Subrahmanyam, S. Saha, A. Govindaraj, H. Krishnamurthy, U. Waghmare, and C. Rao, Adv. Mat. **21**, 4726–4730 (2009).

[9] M. Wu, C. Cao, and J. Jiang, Nanotechnology **21**, 505202–505208 (2010).

[10] C. Zhang, L. Fu, N. Liu, M. Liu, Y. Wang, and Z. Liu, Adv. Mater. **23**, 1020–1024 (2011).

[11] D. Usachov, O. Vilkov, A. Gruneis, D. Haberer, A. Fedorov, V. Adamchuk, A. Preobrajenski, P. Dudin, A. Barinov, M. Oehzelt, C. Laubschat, and D. Vyalikh, Nano Lett. **11**, 5401–5407 (2011).

[12] Y. Wang, Y. Shao, D. Matson, J. Li, and Y. Lin, ACS Nano **4**, 1790–1798 (2010).

[13] A. Reddy, A. Srivastava, S. Gowda, H. Gullapalli, M. Dubey, and P. Ajayan, ACS Nano **4**, 6337–6342 (2010).

[14] L. Qu, Y. Liu, J.-B. Baek, and L. Dai, ACS Nano **4**, 1321–1326 (2010).

[15] J. Perdew, K. Burke, and M. Ernzerhof, Phys. Rev. Lett **77**, 3865–3868 (1996).

[16] H. J. Monkhorst and J. D. Pack, Phys. Rev. B **13**, 5188–5192 (1976).